Construction and Building Materials 122 (2016) 118–125

Contents lists available at ScienceDirect

Construction and Building Materials

journal homepage: www.elsevier.com/locate/conbuildmat

Bacteria-based self-healing concrete to increase liquid tightness of cracks

E. Tziviloglou *, V. Wiktor, H.M. Jonkers, E. Schlangen

Delft University of Technology, The Netherlands

HIGHLIGHTS

- Sealing efficiency of cracks was studied on bio-based self-healing mortar specimens.
- Wet-dry healing treatment favoured the sealing efficiency in bio-based samples.
- Bacterial activity was proven through ESEM observations and O_2 profile measurements.

ARTICLE INFO

Article history:
Received 6 October 2015
Received in revised form 7 June 2016
Accepted 14 June 2016
Available online 22 June 2016

Keywords:
Self-healing
Mortar
Bacteria
Crack sealing
Recovery of water tightness
Permeability test

ABSTRACT

The innovative technology of self-healing concrete allows the material to repair the open micro-cracks that can endanger the durability of the structure, due to ingress of aggressive gasses and liquids. Various concepts of self-healing concrete have been developed, with target on the recovery of water tightness after cracking. Among those, bacteria-based self-healing concrete has shown promising results regarding the improvement of crack sealing performance. In this study, the bacteria-based healing agent is incorporated into lightweight aggregates and mixed with fresh mortar. By this means, autogenous healing of concrete is enhanced and upon cracking the material is capable to recover water tightness. The study focuses on the investigation of the effect of healing agent when incorporated into the mortar matrix and the evaluation of the recovery of liquid tightness after cracking and exposure to two different healing regimes (water immersion and wet-dry cycles) through water permeability tests. It was found that the compressive strength of the mortar containing lightweight aggregates is not affected by the presence of the healing agent. The study also reveals that the recovery of water tightness does not differ substantially either for specimens with or without healing agent when immersed continuously in water. Conversely, the recovery of water tightness increases significantly for specimens containing the healing agent compared to specimens without it, when subjected to wet-dry cycles. Oxygen concentration measurements and bacterial traces on calcite formations confirmed the bacterial activity on specimens containing the healing agent.

1. Introduction

Concrete is a structural material that has been widely used in the modern age [1]. Yet, unavoidable surface micro-cracking can increase the permeability, make it susceptible to aggressive agents and consequently affect the durability of the material [2–4]. Cracking of concrete structures is triggered by temperature and humidity fluctuations, mainly at an early age, and by external loading, mainly at a later age, creating a pathway through which harmful substances enter into the material and decay it gradually over time [4].

It is known that fine cracks, exposed to moist conditions can sometimes close completely [5]. This property, namely autogenous healing, allows the crack to seal through chemical, physical and mechanical processes that take place inside the crack [6]. The mechanisms that cause "crack closure" or "crack bridging" have been known through previous studies [6–8]. However, the most significant factor that influences the autogenous healing is the formation of calcium carbonate ($CaCO_3$) [6]. Scientists more than a decade have worked on various self-healing concrete concepts [4,5], in order to enhance the autogenous healing of concrete. Among the most popular concepts are those which: a) limit the crack width by incorporating fibres [9–13], b) expand the cement matrix when in contact with water by using hydrogels [14,15], c) introduce a healing agent that is activated

* Corresponding author at: Stevinweg 1, 2628CN Delft, The Netherlands.
E-mail address: e.tziviloglou@tudelft.nl (E. Tziviloglou).

http://dx.doi.org/10.1016/j.conbuildmat.2016.06.080
0950-0618/

and released upon cracking [16–24] and d) combine the previous [10–12,25–28].

Recently, bacteria-based self-healing concrete has drawn a lot of attention. The bacteria-based healing agent consists of bacterial spores and organic compounds incorporated into the concrete matrix. The healing agent is encapsulated, in order to immobilize and protect it from crushing during mixing and from the high alkalinity of the cement matrix [16].

In the current study, the bacteria-based healing agent is embedded into lightweight aggregates (LWA). Upon crack formation the weak lightweight capsules break; the healing agent activates and fills the open crack by precipitating $CaCO_3$. Although crack closure can be characterized through visual observations [16,29–31], the functional property of a self-healing material, i.e. the ability to seal the crack and regain water tightness, must be investigated differently. In order to assess the recovery of water tightness (RWT) after cracking and healing, various studies [6,9,29,30,32–33] have developed several crack permeability tests. The aim of this study is to investigate how the addition of the healing agent affects the fresh- and hardened-state properties of the mortar and to evaluate the RWT after cracking and healing through two different healing treatments (water immersion and wet-dry cycles).

2. Materials and methods

2.1. Preparation of the healing agent

The bacteria-based healing agent consisted of spores derived from alkaliphilic bacteria of the genus *Bacillus* and organic mineral compounds. The healing agent is incorporated in LWA (expanded clay particles, Liapor 0/4 mm, Liapor GmbH Germany) via an impregnation under vacuum with calcium lactate (200 g/L), yeast extract (4 g/L) and bacteria spores (10^8 spores/L) solution. Following the impregnation, the LWA were dried for approximately for 5–6 days at standard at temperature (20 ± 2 °C) with (60 ± 10) % RH, until a constant weight was achieved. After drying, the impregnated LWA showed weight increase of approximately 10% [34], comparing to their initial dry weight.

2.2. Preparation of the mortar specimens

Three types of mixtures were investigated. One reference mixture (REF) with normal weight aggregates, one control mixture (CTRL) with non-impregnated LWA and one mixture (B) with impregnated LWA. The mixtures contained ordinary Portland cement (CEM I 42.5 N, ENCI, The Netherlands) and 0/4 mm sand or 0.125/1 mm sand and 1/4 mm LWA. The detailed mixture proportions are presented in Table 1. For the examination of the influence of the healing agent on the fresh- and hardened-state properties of the mortar 9 prisms (40 mm × 40 mm × 160 mm) were cast per mixture. In addition, for the investigation of sealing efficiency of the mortar mixtures, 15 reinforced mortar prisms (40 mm × 40 mm × 160 mm) modified with a hole in their centre, as seen in Fig. 1, were cast per mixture. All specimens were demoulded 24 h after casting and kept in a room with standard temperature (20 ± 2 °C) and >95% RH for 28 days.

2.3. Material characterization, crack introduction and healing on mortar specimens

Immediately after mixing, three fresh-state mortar properties were tested, i.e. consistency, bulk density and air content. The tests and the values obtained were according to EN 1015-3, EN 1015-10 and EN 1015-7 respectively. Flexural and compressive strength was determined on 3-days-, 7-days- and 28-days-old (unreinforced) specimens according to the procedure described at EN 1015-11.

Table 1
Mortar mix designs.

Mixture	CEM I (kg/m^3)	Water (kg/m^3)	0.125/1 mm Sand (kg/m^3)	1/4 mm Sand (kg/m^3)	1/4 mm LWA (kg/m^3)
REF	463	231.5	855	825	0
CTRL	463	231.5	855	0	257
B	463	231.5	855	0	280[1]

[1] This weight includes the weight of impregnated healing-agent into the pores of the LWA.

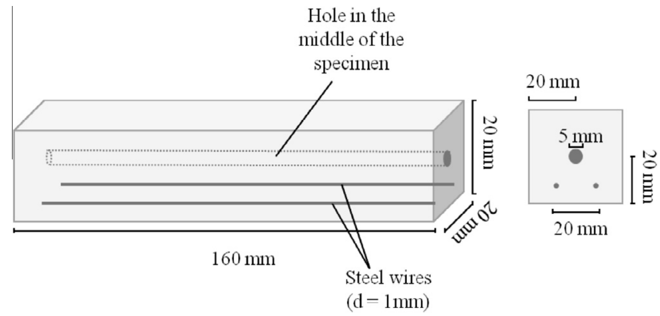

Fig. 1. Specimens for evaluation of RWT.

Damage introduction was performed on 28-days-old reinforced prismatic specimens via 3-point-bending test (Fig. 2). The specimens were loaded until the formation of a single stable and rather large crack (350 μm), without being fractured completely into two parts. Each specimen was placed on the testing machine, where a vertical load was applied at the middle span of the sample, so that the crack opening increased constantly by 0.5 μm/s. When a crack opening of approximately 400 μm was reached, the samples were slowly unloaded. After unloading, the crack width was reduced to approximately 350 μm.

Following the crack creation, 6 specimens of each mixture were placed horizontally in a plastic container filled with tap water for crack healing. The specimens were placed on the top of spacers (10 mm high), so that there was space between them and the bottom of the container. The container was kept open to the atmosphere at standard room temperature (20 ± 2 °C) with (60 ± 10) % RH for 28 or 56 days. Extra water was added (on a weekly basis), to keep a constant liquid-to-solid ratio. Another 6 specimens of each mixture were subjected to wet and dry cycles for 28 or 56 days. The specimens were placed on spacers in plastic containers. Each cycle lasted 12 h. An external pump was either supplying the container with water or was removing it. The container was kept open to the atmosphere at standard room temperature (20 ± 2 °C) with (60 ± 10) % RH.

2.4. Crack water permeability test

The sealing efficiency of the healing agent was initially investigated through stereomicroscopic images. Although stereomicroscopic observations can give an indication, the results should be combined with a crack permeability test in order to link the functional property (water permeability) with the visual observations. The test was performed on three specimens before; and on another three specimens after the healing treatment, according to [33]. Before performing the permeability test and after the healing treatment was completed, one of the two end-sides (40 mm × 40 mm) of the sample was covered with a glue layer to prevent water passage from this side.

Under the crack an electronic scale connected with a computer was recording the weight of the water dripping from the crack as a function of time. Each test lasted approximately 10 min, in order to make sure that the water flow out of the crack was stable. After the completion of the crack permeability tests, the RWT for each set of the three healed specimens was calculated as follows:

$$RWT = \frac{W_{n-h}(t) - W_h(t)}{W_{n-h}(t)}\ x\ 100\% \quad (1)$$

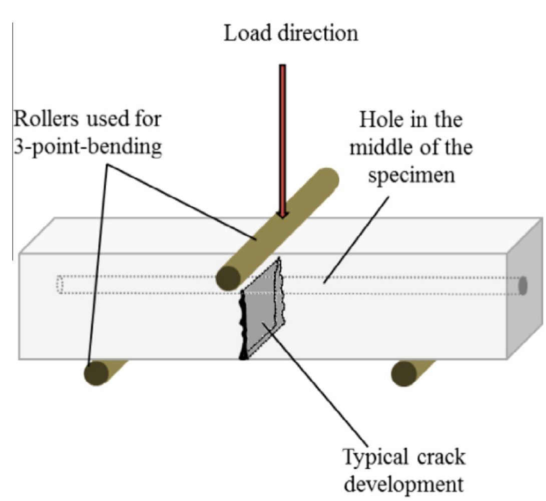

Fig. 2. Three-point-bending set-up.

where $W_{n-h}(t)$: The average (out of three specimens) amount of water that has passed through the unhealed cracks of the specimens in ten minutes (units in g); $W_h(t)$: The average (out of three specimens) amount of water that has passed through the healed cracks of the specimens in ten minutes (units in g).

2.5. Investigation of the healing product inside the crack

For the investigation of the healing product formed inside the crack during healing treatment, the prisms were separated in two parts, so that both crack surfaces were exposed. The morphology of the precipitates was investigated by examination of the crack surface via Environmental Scanning Electron Microscope (ESEM, Philips XL30 Series) equipped with Energy Dispersive X-ray spectrometer (EDS). In addition, Fourier-Transform Infrared (FT-IR) spectrometer (Perkin-Elmer Spectrum 100 Series equipped with Attenuated Total Reflexion) was used for identification of the precipitates (2–3 g) scrapped from the crack surface. The spectra obtained after 16 scans with a resolution of 2 cm^{-1} in the range of 4000–600 cm^{-1}.

2.6. Oxygen consumption measurements

The concept of the bacteria-based self-healing concrete indicates that in the presence of oxygen and water inside the crack, the dormant bacterial spores are activated. Later, the active bacteria cells convert the calcium lactate ($CaC_6H_{10}O_6$), present in the healing agent to $CaCO_3$ (see Eq. (2)) by using oxygen [16].

$$CaC_6H_{10}O_6 + 6O_2 \rightarrow CaCO_3 + 5CO_2 + 5H_2O \quad (2)$$

Therefore, by conducting oxygen concentration measurements on samples submerged in water and in alkaline solution, it was possible to trace bacterial activity in the samples with healing agent. For this test micro-sensor type Oxy50M (Presens, Germany) was used. The measurements were performed on the exposed crack surface of the specimens. The micro-sensor, fixed to a motorized micromanipulator for the vertical axis, was measuring the oxygen concentration in vertical steps of 50 μm from 5 mm above, down to the surface of the specimen, placed in a 4 L-water tank filled either with tap water or with carbonate-bicarbonate buffer (0.1 M, pH = 10.5) at 20 ± 2 °C. Each set of measurements ran for 10 min and then after 10 min the next set was starting (3 tests/h). After the completion of the test, which lasted for 5 h for the specimens in water and 9 days for the specimens in buffer, oxygen micro-profile measurements were obtained.

The schematic representation of the complete experimental procedure that was followed during this research is depicted in Fig. 3.

3. Results

3.1. Fresh- and hardened-state properties of mortar prisms

The effect that the healing agent has on the cementitious material was examined through the comparison of several properties of the mixtures with- and without healing agent. The comparison was conducted in two steps; first on fresh mixtures and then on hardened prisms. Table 2 presents the results obtained by the tests performed on the fresh mixtures. The tests revealed that the replacement of sand with LWA leads to substantial decrease of the bulk density and tends to increase the air content, while it hardly affects the consistency of the fresh mixture. Furthermore, the presence of the healing agent seems to affect all of the above-mentioned characteristics leading in a lighter and more flowable mixture. Fig. 4 shows the results obtained by flexural and compressive tests on hardened prisms. The tests revealed that the healing agent affects significantly the hardened properties of the mixture at the age of 3 days, leading in a weaker material. However, after the age of 7 days the flexural strength of all three types of mixtures falls in the same range. In addition, the compressive strength of specimens with NWA is constantly higher at all ages (3, 7 and 28 days) compared to the other two mixtures with LWA. Moreover, both CTRL and B mixtures show a quite similar compressive strength after the age of 7 days.

3.2. Recovery of water-tightness and healing product investigation

The efficiency of the healing agent was investigated initially through stereomicroscopic images and later through crack permeability tests. Fig. 5 shows typical examples of cracks before and after each healing treatment. The stereomicroscopic images revealed that REF and CTRL specimens that were immersed in water for 28 or 56 days showed partial or full crack closure, but when subjected to wet-dry cycles the healing was substantially less or even non-existent. On the other hand, the cracks of B

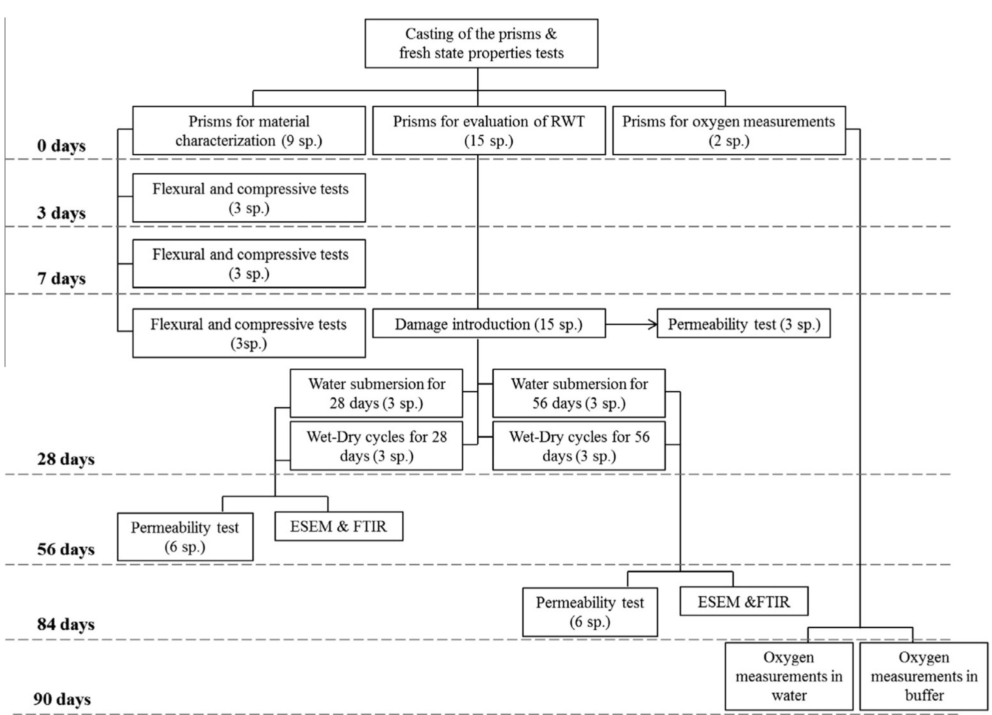

Fig. 3. Schematic representation of the experimental procedure (sp. stands for specimens).

Table 2
Fresh state properties of mortar mixtures.

Property	REF	CTRL	B
Flow (mm)	145	155	185
Density (kg/m^3)	2192	1652	1546
Air content (%)	5	8	14

specimens that were immersed in water for 28 or 56 days exhibited obviously improved crack closure, compared to REF and CTRL specimens subjected to the same healing treatments. Furthermore, the cracks of B specimens which were exposed to wet-dry cycles demonstrated complete crack closure in almost all cases.

Fig. 6 shows the average (out of 3 specimens) RWT of the three types of prismatic specimens. The results are in good agreement with the stereomicroscopic observations. In fact, the specimens without healing agent show a relatively high RWT when immersed under water, i.e. 71% and 80% for the REF specimens and 31% and 82% for the CTRL specimens, for healing treatment of 28 and 56 days respectively. Very similar was also the behaviour of B specimens under water. The RWT was 69% for 28 days and 91% for 56 days of water submersion. The results differed for the specimens that were subjected to wet-dry cycles. The specimens without healing agent exhibited considerably lower RWT when

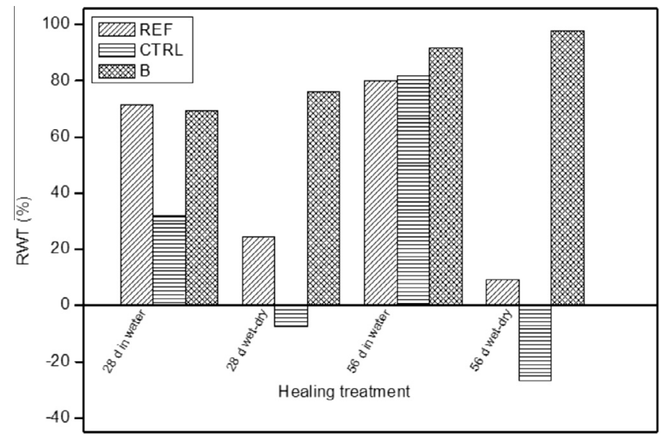

Fig. 6. Average RWT in specimens subjected to 28 and 56 days healing treatment.

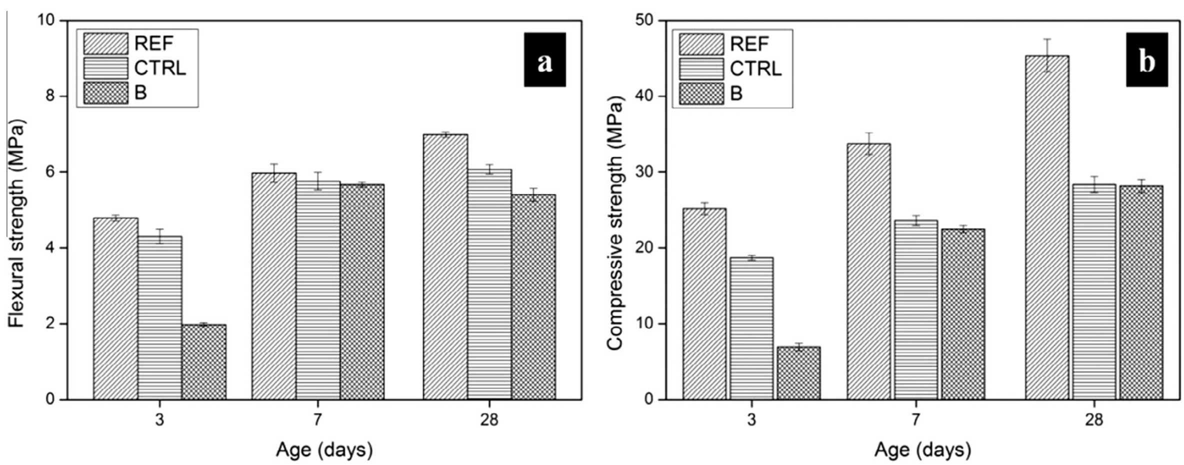

Fig. 4. a. Average flexural strength of prismatic specimens at 3, 7 and 28 days and b. Average compressive strength of prismatic specimens at 3, 7 and 28 days.

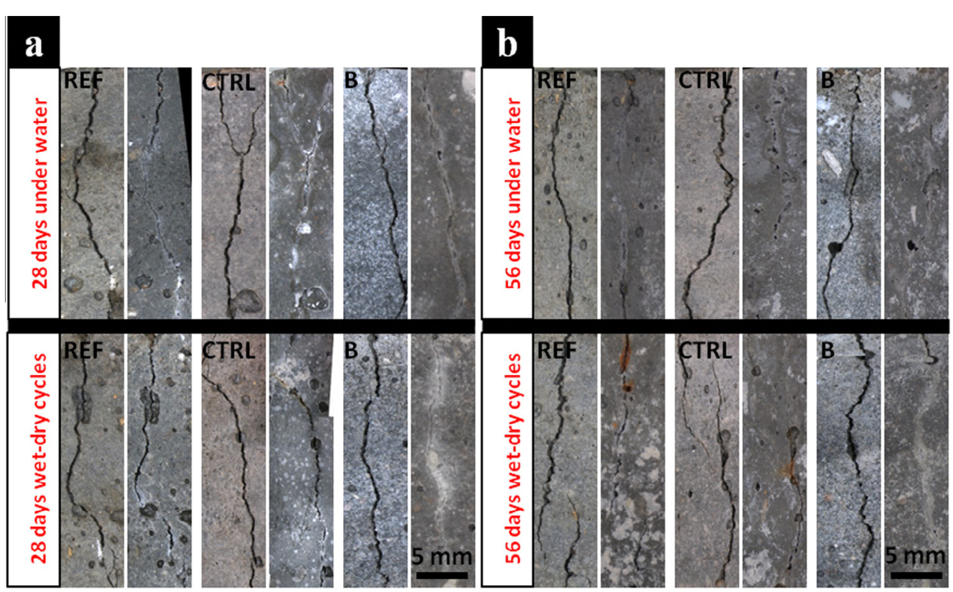

Fig. 5. a. Typical stereomicroscopic observations of cracks subjected to 28 days of healing treatment b. Typical stereomicroscopic observations of cracks subjected to 56 days of healing treatment.

compared to REF and CTRL specimens under water. Especially, for CTRL specimens subjected to wet-dry cycles the flow of water out of the crack was even higher than the flow before the healing treatment (negative values). On contrary, the RWT on B specimens subjected to wet-dry cycles reached 76% for 28 days and 98% for 56 days healing treatment.

ESEM observations revealed that the main crystal shapes that were found in the cracks of the three different types of mortar samples were in almost all cases either cubic or clustered asymmetric rhombohedral, possibly formations of $CaCO_3$. Fig. 7 shows typical formations lying on the surfaces of the cracks that were found by ESEM observations. During the 28 days of healing treatment on REF and CTRL samples the crystals that were created were considerably smaller than those formed in the cracks of B specimens. Despite the larger size, small holes and cavities (1–2 μm wide, ~5 μm long) similar to bacterial imprints were observed on the surface of the crystals found in B specimens. After 56 days of healing treatment the crystals created inside the cracks of REF and CTRL specimens were fairly larger compared to those of 28 days treatment, yet smaller than the crystals in B specimens. However, this time the surface of the precipitates found in B specimens was rather smooth. The EDS analysis on the abovementioned crystalline formations indicated high peaks of Ca, C and O, which suggested that indeed $CaCO_3$ was present.

The Fourier-Transform Infrared (FT-IR) spectra revealed very similar peaks for the three different types of specimens. In fact,

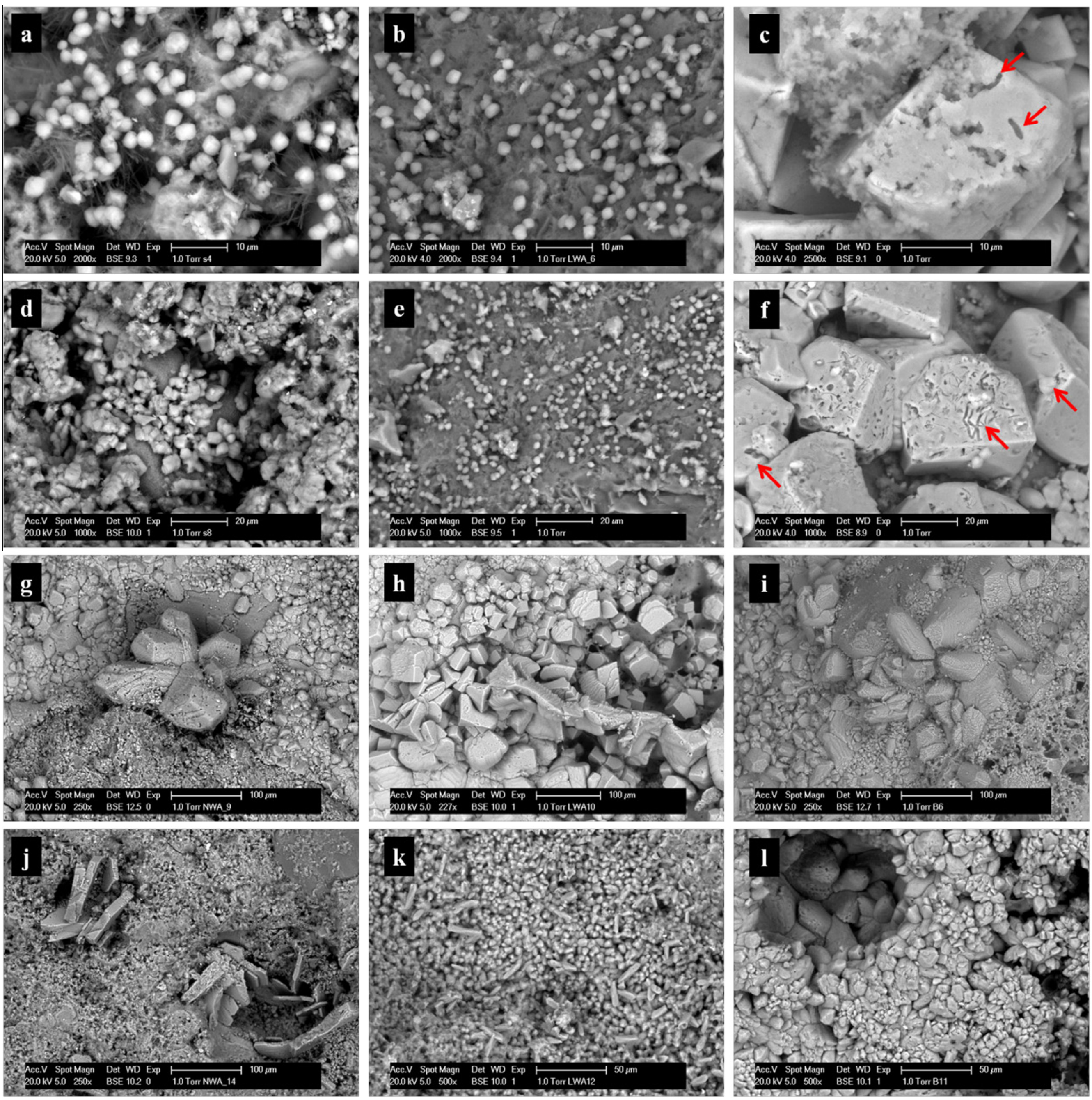

Fig. 7. ESEM images of precipitates that were found on the surface of the crack after healing treatments a. REF specimen, b. CTRL specimen, c. B specimen submerged in water for 28 days; d. REF specimen, e. CTRL specimen, f. B specimen subjected to wet-dry cycles for 56 days; g. REF specimen, h. CTRL specimen, i. B specimen submerged in water for 28 days; j. REF specimen, k. CTRL specimen, l. B specimen subjected to wet-dry cycles for 56 days.

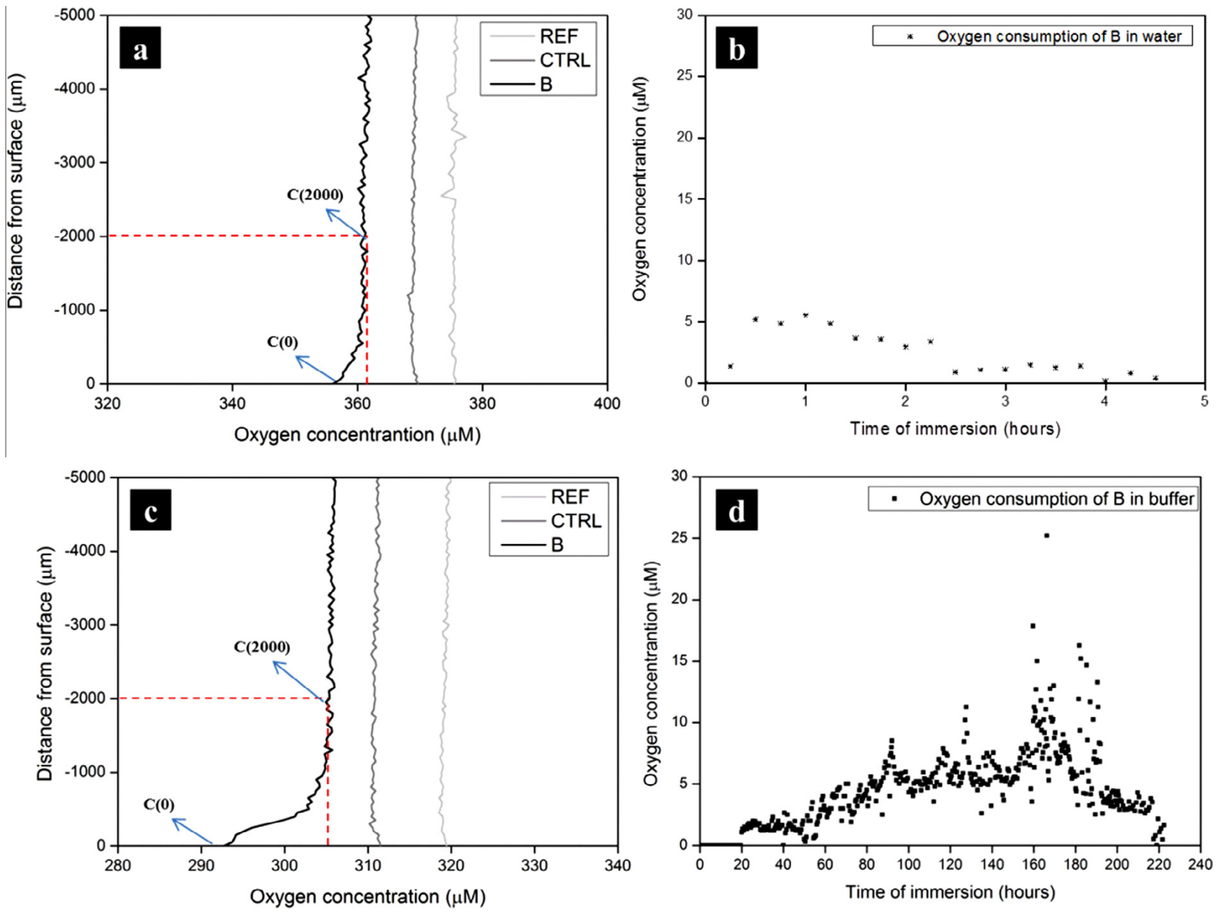

Fig. 8. a. Typical profile obtained by specimens in tap water, b. Oxygen consumption in time from B specimen immersed in tap water c. Typical profile obtained by specimens in buffer, d. Oxygen consumption in time from B specimen immersed in buffer.

all spectra exhibited strong calcite bands that appear at around wave numbers 1400 cm^{-1}, 870 cm^{-1} and 712 cm^{-1}, typical of carbonate vibrations in calcite, and some weaker bands at 2511 cm^{-1} and at 1796 cm^{-1} [35–37].

3.3. Oxygen concentration measurements

Oxygen profile measurements showed that oxygen consumption existed only for the specimens that contained the bacteria-based self-healing agent. For REF and CTRL specimens the profiles obtained were rather straight along the measuring distance, while the profiles derived from B specimens were stable until 500 µm above their surface, where they obviously started constantly to decrease. Fig. 8a and c shows typical oxygen profiles obtained by specimens immersed in tap water and in carbonate-bicarbonate buffer respectively. Although, there was oxygen consumption in both liquids (tap water and buffer); the starting time, the duration and the magnitude of consumption were different. In fact, for the B specimen in tap water the consumption started almost immediately after immersion, it lasted approximately 2.5 h and the highest value reported was 5,5 µM at 1 h after the immersion. For the B specimen in carbonate-bicarbonate the consumption started after 20 h of immersion, it lasted approximately 8 days and the highest value reported was 26 µM at 170 h after the immersion. Fig. 8b and d shows the oxygen consumption in time for B specimen submerged in tap water and in carbonate-bicarbonate buffer respectively. The values on Fig. 8b and d were obtained by subtracting the oxygen concentration value on the surface of the specimen (C(0)) from the oxygen concentration value at 2000 µm above the surface of the specimen (C(2000)).

4. Discussion

The results of this study revealed that replacement of sand with LWA in the mortar specimens led to considerable reduction of the density and the compressive strength of the cementitious material, as expected. The incorporated healing agent created a rather liquid fresh mixture with increased air content, but it also delayed the hardening of the cement approximately one day. As a consequence, the early age (3 days) flexural and compressive strength of the B prisms was 54% and 63% respectively, lower compared to the CTRL specimens. Yet, at a later age (>7 days) the healing agent presence does not seem to affect the hardened properties, i.e. the flexural and the compressive strength of the material.

Another main focus of this paper was to investigate whether the autogenous healing can be enhanced due to the addition of the bacteria based self-healing agent in mortar. This investigation was carried out through water permeability experiments on cracked mortar prisms exposed to two different healing regimes. The results showed that there was indeed reduction of the initial water flow from the cracks of REF and CTRL specimens that were submerged under water for 28 as well as 56 days. This reduction can be attributed to the autogenous healing mechanisms/reactions that can take place during water immersion. On the other hand, the same type of specimens exhibited substantially lower RWT when exposed to wet-dry cycles. The same behaviour has been reported by Roig-Flores et al. [38], who proved through water permeability tests that concrete samples immersed in water achieved higher healing rates than samples exposed to wet-dry cycles. B specimens showed similar RWT results with REF and CTRL specimens, when immersed in water. However, the differentiation in RWT of the specimens containing the bacteria-based healing agent is well emphasized by the significantly higher values obtained by specimens that were subjected to wet-dry cycles. The higher concentration of oxygen in the air during dry cycle seems to promote the bacterial activity leading in increased amount of $CaCO_3$ precipitates.

Traces of bacterial activity were found on the surfaces of the crystals formed inside the cracks of B specimens that were exposed for 28 days to complete water immersion or to wet-dry cycles. The shape and the size of holes and cavities that were observed are very similar to those described in the literature [39–43], as bacteria imprints on microbially induced calcium carbonate precipitates. However, those imprints could not be found on crystals after 56 days of healing treatment, possibly due to the fact that the crystals gradually grow in time [44] and can cover the bacterial traces.

The oxygen concentration profiles were used as a supplementary tool to investigate the existence of bacterial activity on the mortar specimens with the bacteria-based healing agent. The results of experiments on B specimens submerged in tap water showed that the consumption of oxygen near the surface of the crack was lower and lasted less than in B specimens submerged in carbonate-bicarbonate buffer. The explanation may lie on two facts:

a) The bacteria that exist in the tap water are already active, vegetative cells that they find the organic compound incorporated in the healing agent and start to metabolize it immediately after the immersion of the specimen. On contrary, when the sample is immersed in the buffer the bacteria possibly contained in the water that was used for the preparation of the buffer solution are not active due to the high alkalinity. Therefore, the recorded oxygen consumption is caused only from the bacteria incorporated into the healing agent. Since those bacteria need some time to turn in from dormant to active state, the consumption is delayed.
b) The solubility of calcium lactate in water is rather high [45], consequently it can dissolve very fast in the bulk water. During this study, it was observed that calcium lactate was dissolving quite slow in the buffer solution. Thus, the healing agent can stay for longer period undissolved at the same place until bacterial spores are activated and start the metabolic activity.

5. Conclusion

In conclusion, the lightweight mortar with incorporated bacteria-based healing agent shows improved crack sealing, particularly when subjected to a more realistic healing regime, i.e. wet-dry cycles, than continuous water immersion. The proof that this enhanced behaviour is coming from the bacterial activity is supported by oxygen consumption measurements and ESEM observations. The replacement of normal weight sand by lightweight aggregates, leads in a reduction of the compressive strength of the bacteria-based mortar. Yet, this material could be used where a lightweight structure is needed, or as an external layer on a normal weight structure. Overall, it could be stated that structures can benefit from the use this material, since the enhanced crack sealing behaviour can prevent durability problems that are related with micro-cracking.

Acknowledgements

The authors acknowledge the financial support of European Union Seventh Framework Programme (FP7/2007-2013) under grant agreement n° 309451 (HEALCON), Mr. Arjan Thijssen and Mr. Gerrit Nagtegaal for the technical support.

References

[1] H.G. van Oss, Background Facts and Issues Concerning Cement and Cement Data, U.S. Department of the Interior and U.S Geological Survey, 2005.
[2] A.F. Karr, C.-M. Aldea, S.P. Shah, Effect of microcracking on durability of high-strength concrete, Paper No. 99-0801, Transp. Res. Rec. 1668 (1999) 86–90.
[3] Z. Yang, W.J. Weiss, W.J. Olek, Interaction Between Micro-Cracking, Cracking, and Reduced Durability of Concrete: Developing Methods for Considering Cumulative Damage in Life-Cycle Modeling, Report No.: Publication FHWA/IN/JTRP-2004/Joint Transportation Research Program, 2005. West Lafayette, Indiana.
[4] E. Schlangen, C. Josef, Self-healing processes in concrete, in: S.K. Gosh (Ed.), Self-Healing Materials: Fundamentals, Design Strategies, and Applications, Wiley-VCH verlag GmbH and Co KGaA, 2009, pp. 141–182.
[5] M. De Rooij, K. Van Tittelboom, N. De Belie, E. Schlangen, Self-healing Phenomena in Cement-Based Materials, State-of-the-art Report of RILEM Technical Committee, 2012.
[6] C. Edvardsen, Water permeability and autogenous healing of cracks in concrete, ACI Mater. J. Am. Concr. Inst. 96 (1999) 448–454.
[7] N. Hearn, Self-sealing, autogenous healing and continued hydration: what is the difference?, Mater Struct. 31 (8) (1998) 563–567.
[8] N. Ter Heide, E. Schlangen, K. van Breugel, Experimental Study of Crack Healing of Early Age Cracks, Technical University of Denmark, Denmark, 2005, p. 2005.
[9] Y. Yang, M.D. Lepech, E.-H. Yang, V.C. Li, Autogenous healing of engineered cementitious composites under wet–dry cycles, Cem. Concr. Res. 39 (2009) 382–390.
[10] V.C. Li, Y.M. Lim, Y.W. Chan, Feasibility of a passive smart self-healing cementitious composite Composites B, 29B, Composites Part B 29 (6) (1998) 819–827.
[11] E. Tziviloglou, Self-Healing in ECC Materials with Low Content of Different Microfibres and Micro-Particles, Delft University of Technology, 2009.
[12] S. Antonopoulou, Self-Healing in ECC Materials with High Content of Different Microfibres and Micro-Particles, Delft University of Technology, 2009.
[13] Z. Zhang, S. Qian, H. Ma, Corrigendum to "Investigating mechanical properties and self-healing behavior of micro-cracked ECC with different volume of fly ash", Constr. Build. Mater. 52 (2014) 17–23.
[14] J.S. Kim, E. Schlangen, Super Absorbent Polymers to Simulate Self Healing in ECC, RILEM Publications S.A.R.L., 2010, pp. 849–858.
[15] D. Snoeck, K. Van Tittelboom, N. De Belie, The use of superabsorbent polymers as a crack sealing and crack healing mechanism in cementitious materials, 2012, pp. 152–157.
[16] V. Wiktor, H.M. Jonkers, Quantification of crack-healing in novel bacteria-based self-healing concrete, Cement Concr. Compos. 33 (2010) 763–770.
[17] H.M. Jonkers, Bacteria-based self-healing concrete, HERON 56 (1) (2011) 1–12.
[18] T. Nishiwaki, H. Mihashi, B.-K. Jang, K. Miura, Development of self-healing system for concrete with selective heating around crack, J. Adv. Concr. Technol. 4 (2) (2006) 267–275.
[19] H. Mihashi, Y. Kaneko, T. Nishiwaki, K. Otsuka, Fundamental study on development of intelligent concrete characterized by self-healing capability for strength, Trans. Jpn. Concr. Inst. 22 (2000) 441–450.
[20] C.M. Dry, Three designs for the internal release of sealants, adhesives, and waterproofing chemicals into concrete to reduce permeability, Cem. Concr. Res. 30 (2000) 1969–1977.
[21] S. Sangadji, E. Schlangen, Self healing of concrete structures, novel approach using porous network concrete, J. Adv. Concr. Technol. 10 (5) (2012) 185–194.
[22] R. Mors, H.M. Jonkers, Reduction of Water Permeation through Cracks in Mortar by Addition of Bacteria based Healing Agent, 2015 Jun 22–2015 Jun 24, 2015.
[23] K. Van Tittelboom, N. De Belie, D. Van Loo, P. Jacobs, Self-healing efficiency of cementitious materials containing tubular capsules filled with healing agent, Cement Concr. Compos. 33 (4) (2011) 497–505.
[24] W. De Muynck, D. Debreouwer, N. De Belie, W. Verstraete, Bacterial carbonate precipitation improves the durability of cementitious materials, Cem. Concr. Res. 38 (7) (2008) 1005–1014.
[25] D. Snoeck, K. Van Tittelboom, Stijn Steuperaert, Peter Dubruel, N. De Belie, Self-healing cementitious materials by the combination of microfibres and superabsorbent polymers, J. Intell. Mater. Syst. Struct. 25 (1) (2012) 13–24.
[26] S. Sangadji, Porous Network Concrete: A Bio-Inspired Building Component to Make Concrete Structures Self-Healing, Delft University of Technology, 2015.
[27] J. Wang, D. Snoeck, W. Verstraete, N. De Belie, Application of hydrogel encapsulated carbonate precipitating bacteria for approaching a realistic self-healing in concrete, Constr. Build. Mater. 68 (2014) 110–119.
[28] M.G. Sierra Beltrαn, H.M. Jonkers, W. Mera Ortiz, Concrete with Abaca Fibres and Bacteria to Improve Sustainability and Performance of Irrigation Canals in Ecuador, 2013 Jun 9–2013 Jun 11, 2013.

[29] K. Van Tittelboom, E. Gruyaert, H. Rahier, N. De Belie, Influence of mix composition on the extent of autogenous crack healing by continued hydration or calcium carbonate formation, Constr. Build. Mater. 37 (349) (2012) 359.
[30] M. Roig-Flores, S. Moscato, P. Serna, L. Ferrara, Self-healing capability of concrete with crystalline admixtures in different environments, Constr. Build. Mater. 86 (2015) 1–11.
[31] D. Palin, V. Wiktor, H.M. Jonkers, Autogenous healing of marine exposed concrete: characterization quantification through visual crack closure, Cem. Concr. Res. 73 (17) (2015) 24.
[32] H.W. Reinhardt, M. Jooss, Permeability and self-healing of cracked concrete as a function of temperature and crack width, Cem. Concr. Res. 33 (981) (2003) 985.
[33] E. Tziviloglou, H.M. Jonkers, E. Schlangen, Bacteria-based Self-Healing Concrete to Increase Liquid Tightness of Cracks, 2014 May 26–2014 May 28, 2014, pp. 650–655.
[34] E. Tziviloglou, V. Wiktor, H.M. Jonkers, E. Schlangen, Optimization of Incorporation Procedure of Bio-based Healing Agent into Light Weight Aggregates, 2015 Jun 22–2015 Jun 24, 2015.
[35] F.A. Miller, C.H. Wilkins, Infrared spectra and characteristic frequencies of inorganic ions, Anal. Chem. (1952) 1253–1294.
[36] C. Pelosi, G. Agresti, M. Andaloro, P. Baraldi, P. Pogliani, U. Santamaria, The rock hewn wall paintings in Cappadocia (Turkey), in: Characterization of the Constituent Materials and a Chronological Overview, 2012 Mar 28–2012 Mar 31, 2012, pp. 99–108.
[37] V. Ramachandran, J.J. Beaudion, Handbook of Analytical Techniques in Concrete Science and Technology, Principles Techniques and Applications, Noyes Publications, New York, 2001.
[38] M. Roig-Flores, F. Pirritano, P. Serna, L. Ferrara, Study of the Self-Healing Behavior of Early-Age Cracks in Concrete with Crystalline Admixtures Under six Environmental Exposures, 2015 Jun 22–2015 Jun 24, 2015.
[39] S. Stocks-Fischer, J.K. Galinat, S.S. Bang, Microbiological precipitation of $CaCO_3$, soil biology and biochemistry, Soil Biol. Biochem. 31 (1999) 1563–1571.
[40] P. Cacchio, C. Ercole, G. Cappucio, A. Lepidi, Calcium carbonate precipitation by bacterial strains isolated from a limestone cave and from a loamy soil, Geomicrobiol. J. 20 (2) (2003) 85–98.
[41] S.A. Abo-El-Enein, A.H. Ali, F. Talkhan, H.A. Abdel-Gawwad, Utilization of microbial induced calcite precipitation for sand consolidation and mortar crack remediation, HBRC J. 8 (2012) 185–192.
[42] J. Polka, P.A. Silver, Induced sensitivity of *Bacillus subtilis* colony morphology to mechanical media compression, Peer J. (2014).
[43] N.K. Dhami, A. Mukherjee, Can we Benefit from the Microbes Present in Rammed Earth?, CRC Press, 2015, pp 89–92.
[44] S. Baskars, R. Baskar, L. Mauclaire, J.A. McKenzie, Microbially induced calcite precipitation in culture experiments: possible origin for stalactites in Sahastradhara caves, Dehradun, India, Curr. Sci. 90 (1) (2006) 58–64.
[45] X. Cao, H.-J. Lee, H.S. Yun, Y.-M. Koo, Solubilities of calcium and zinc lactate in water and water–ethanol mixture, Korean J. Chem. Eng. 18 (1) (2001) 133–135.